EPJ Web of Conferences **320**, 00010 (2025) https://doi.org/10.1051/epjconf/202532000010
CALOR 2024

Design of a 2D Calorimeter Array for Measurement of Radiation Therapy Treatment Beams

Jacob Lambeck [1*], *Jeffrey L.* Radtke[1], and *Larry A.* DeWerd[1]

[1]University of Wisconsin – Madison/UWMRRC, Madison, WI, United States

Abstract. In the field of Medical Physics, calorimeters are often used as an absolute dose measurement in standards labs as part of the chain of calibrations for radiation therapy treatment machines in hospitals and cancer centers. Currently, every calorimeter designed for this purpose is either position-insensitive or 1-dimensional, despite the radiation dose deposited not always being homogeneous across the entire irradiated area. Therefore, a 2-dimensional, position-sensitive, calorimeter array is being designed to provide information on the dose both on the central axis of the radiation beam as well as the dose fall off away from center. The device is composed of 9 voxels in a 3x3 configuration. Each voxel contains a cylindrical core made of high-purity aluminum which is the volume of interest for heating measurements and therefore dose determination. Each core is surrounded by alternating shells of solid Aerogel insulation and additional high-purity aluminum. The outer aluminum shell is operated isothermally with a set temperature above what the ambient air could reach. This provides a buffer for each core from both air temperature fluctuations and heat flow between voxels during measurements. The inner aluminum shell and the core maintain a quasi-adiabatic state to prevent heat flow into or out of the core except from the energy deposited from the radiation. Both temperature measurements and necessary heating for the quasi-adiabatic or isothermal conditions are accomplished using embedded thermistors connected to a LabJack T7 data acquisition (DAQ) device operated by a purpose-built Python control code. The calorimeter array is currently being constructed for testing later this year.

1 Introduction

In early 2024, the World Health Organization estimated that about 20% of the world population will develop cancer in their lifetime [1]. While access to radiation therapy equipment and facilities varies greatly between populations, in the United States, it is estimated that over 50% of patients with aggressive cancers will receive radiation therapy (radiotherapy) as part of their treatment [2].

The biological endpoints of radiation therapy, including the Tumor Control Probability, a metric for determining the likelihood of killing the cancerous tumor, and the Normal Tissue Complication Probability, a metric for determining the likelihood of causing damage to surrounding healthy tissue, are determined based on the radiation dose a target in the body received. This radiation dose is in units of Gray (Gy) and is defined as the energy deposed in the target in joules divided by the mass of the target in kilograms:

$$\text{Dose (Gy)} = \frac{\text{Energy (J)}}{\text{Mass (kg)}} \tag{1}$$

There are many common radiation detectors (also known as dosimeters) which are used to determine dose including ionization chambers, solid-state diodes, radiochromic film, and thermoluminescent dosimeters (TLDs). However, all of these detectors are ‘reference dosimeters’ meaning they require a calibration against a previously calibrated dosimeter or in a well-characterized field of ionizing radiation. There exists, however, another class of dosimeters known as ‘absolute dosimeters’ which are calibrated only against non-radiation standard quantities such as heat or chemical changes and can provide lower dose uncertainty than most reference dosimeters.

1.1 Calorimeters in radiation therapy

When radiation deposits energy into an object, the object experiences a rise in temperature as described by the heat transfer equation:

$$E = m \cdot c_p \cdot \Delta T \tag{2}$$

Where E is the energy absorbed by the object, m is the object’s mass, c_p is the specific heat capacity of the object, and ΔT is the increase in temperature.

By combining this equation with equation 1, we can relate the radiation dose deposited in the object and the object’s change in temperature:

$$D = c_p \cdot \Delta T \cdot \prod_i k_i \tag{3}$$

---

[*] Corresponding author : jlambeck.medphys@gmail.com

Where each k_i is a correction factor that accounts for non-ideal measurement conditions such as conductive heat transfer and radiation field perturbation.

Calorimeters are the most common absolute dosimeter and are used as the primary radiation standard at over 10 national standards labs around the world. These calorimeters measure a temperature change either in a volume of water or graphite [3]. However, all these measurements are position-insensitive or one-dimensional, and there are currently no methods to do absolute dosimetry in multiple dimensions [4].

2 Design of the 2D calorimeter

2.1 Structural design

To maintain spatial independence, the calorimeter is designed as an array of 9 separate voxels arranged in a 3x3 configuration. Each of the voxels are structured as a series of cylindrical shells surrounding a solid cylinder. This inner cylinder is called the core and is the volume of interest where temperature measurements will be taken. Surrounding the core are alternating layers of insulation and two cylindrical shells made of the same material as the core. The inner shell is called the jacket, and the outer shell is called the shield. The concentric shell design is shown in Figure 1a, displaying the alternating pattern of the core, jacket, and shield with layers of thermal insulation.

This layered cylindrical design is common for solid calorimeters in medical physics and allows for better thermal control and easier machining than other shapes [5-7]. Surrounding the shield is additional insulation to form a square boundary for each voxel. Once all of the voxels have been constructed, they will be arranged into the 3x3 configuration, and a solid casing made of a similar material to the core will be placed around the array for support and protection as shown in Figure 1b.

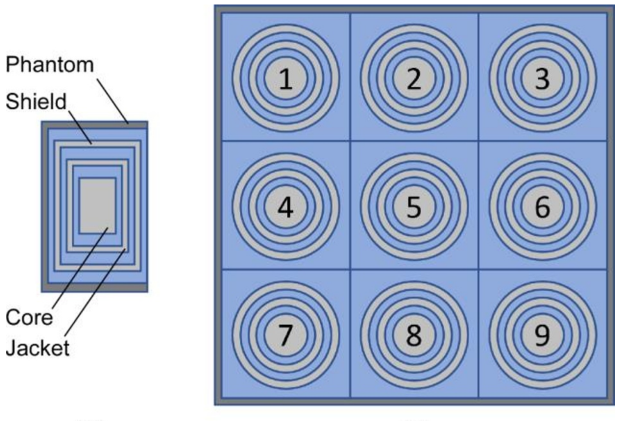

(A) (B)

Fig. 1. Section views of calorimeter. (A) Single voxel, parallel to beam axis, showing layers of high purity aluminum (grey), insulation (blue), and aluminum alloy 6061 (dark grey). (B) Full array, perpendicular to beam, showing numbered voxel locations.

While there are various particles and beam qualities that are used for radiotherapy, the most common are megavoltage photons, electrons, and protons. As temperature increases of 1-2 mK are common for radiotherapy calorimeters, a primary concern with multiple cores is if the signal differences from adjacent cores will be large enough to overcome the noise to yield a noticeable change in measured dose. As such, for this first proof-of-concept design, the array will be tested in a 6 MeV unflattened photon beam as this has the greatest dose difference across the field of any standard treatment beam while also a low enough energy to not have neutron production. For all simulations, a 6FFF phase space source for the Varian TrueBeam linear accelerator was used as the radiation source, with a maximum photon energy of 6 MeV and average photon energy of about 1.7 MeV (Varian Medical Systems, Palo Alto, CA).

2.2 Material selection

Most solid calorimeters have a core made of a high-purity graphite, chosen for its inherent similarity to carbon-based human tissue. This helped to reduce the magnitude of corrections needed to convert from the measured dose-to-graphite to the desired dose-to-water or dose-to-tissue. However, the granular structure of bulk graphite can be highly heterogeneous, due to voids formed through the sintering production process, wherein powder is fused by compression. This makes it difficult, if not impossible, to accurately model bulk graphite computationally [8]. Advancements in Monte Carlo simulation codes have allowed the usage of various pure but less intrinsically human-like materials. Bulk, high-purity aluminium is solidified from a molten state, forming a polycrystalline material with void-free grain boundaries. This relatively homogeneous material has similar thermal properties to graphite but can be more accurately modelled. Therefore, high-purity aluminium was chosen as the material for the core, jacket, and shield.

To make sure the aluminium layers would remain physically separated, the insulation layers need to also be solid, rather than gaps of air or vacuum. Airloy™ is a type of Aerogel that is machinable, comes in various densities, and has very good thermal insulation properties (Aerogel Technologies, LLC, Hyde Park, MA). Airloy X103M was chosen as it has the best insulation properties of the Airloys that are machinable in-house.

For the solid casing around the insulation squares to contain the entire array, a material similar to the core is preferable as it reduces radiation beam perturbation effects. Aluminium alloy 6061 was chosen as it has good machinability, is low cost, has high structural integrity, and is readily available from numerous manufacturers.

To measure the change in temperature caused by an irradiation, temperature sensors must be embedded in the calorimeter. Thermistors are resistors that experience a change in their resistance with a change in temperature, and small, glass bead, negative temperature coefficient (NTC) thermistors that lower their resistance as temperature increases have been used in a wide variety of radiotherapy calorimeters [5, 9-10]. The NTC thermistors used in the calorimeter array are embedded in the core, jacket, and shield and function as both temperature sensors and Joule heaters for distinct purposes in each aluminium component which will be described later.

As mentioned in section 1.1, various correction factors are needed to account for non-ideal measurement conditions. Two of these, the Radiation Field Perturbation and the Dose to Water Conversion factors account for non-aluminium materials in the beam. This includes the Aerogel, casing, and the various materials present in the thermistors. These corrections are calculated using Monte Carlo simulations and are described in more detail in the works of Renaud *et al.* [6].

2.3 Array Sizing

As every component of the array is built out from the core, determining the core size is the most important. A common way this has been done is by looking at the surface area to volume ratio (SA:V) of the core [6, 11]. A large surface area allows for more heat flow out of the core which is bad as this would be energy that was deposited into the core but did not contribute to increasing the core's temperature and thus to the dose determination. A large volume, however, increases the region where radiation particles can interact with the core, giving a higher signal. In addition, a small radius overall is preferable as this allow voxels to be more closely spaced, giving better spatial resolution. The equation for the SA:V of a cylinder is shown in Equation 4 and shows that by increasing either the radius or the height, the ratio will decrease:

$$SA\!:V_{cyl} = \frac{2(R+H)}{R \cdot H} \tag{4}$$

Where R and H are the radius and height of the cylinder, respectively.

However, the cylinder's radius could not be made indefinitely small, as machining difficulties for the Airloy™ insulation prevented the core's radius from being smaller than 3 mm.

Table 1. Comparisons of the dose per incident radiation particle and SA:V for cores of different heights measured through egs_chamber simulations. All cores had radii of 3 mm. Dose per particle does not change greatly with height changes.

Core Height	Dose per incident particle (Gy)	SA:V
6 mm	2.64E-18	10
9 mm	2.65E-18	8.9
10 mm	2.66E-18	8.7

Simulations were performed in the egs_chamber user code of the EGSnrc Monte Carlo code to determine the effect of changing the core's height. Ultimately, it was found that increasing the height does reduce the SA:V and gives higher signal as expected, but the change in dose deposited per incident radiation particle was negligible as shown in Table 1, implying that particles that interacted with the core deposited the bulk of their energy quickly. Ultimately, a core size of 3 mm radius x 9 mm height was chosen as this yields a core volume similar to the active air volume of an Exradin A12S ionization chamber, potentially allowing for additional comparison tests between the two dosimeters, if desired. Ionization chambers like the A12S are the most common dosimeter used in radiation therapy clinics, and comparing to a conventional detector like this is standard practice when introducing a new dosimeter.

For the jacket, shield, and insulation layers, machining constraints limited their thickness to 1 mm at minimum. For the insulation outside of the shield which is used to form the square sides of each voxel, smaller side lengths provide better spatial resolution, but enough insulation is needed to prevent heat flow between voxels during an irradiation measurement. Using the heat transfer module in COMSOL Multiphysics® (COMSOL Inc, Burlington, MA), the heat flow can be modelled during a simulated irradiation on arrays with different voxel side lengths. Lengths between 15 mm and 24 mm were tested, corresponding to 1 mm to 10 mm of insulation between the closest points of shields from adjacent voxels. Figure 2 shows the temperature change from baseline during a simulated irradiation where only the central voxel was irradiated, and the voxel side length is minimized at 15 mm. This simulates a worst-case scenario as with only a single voxel being heated, the temperature gradient between that voxel and adjacent ones is the greatest and would therefore have the most heat flow. As measurements are only taken during irradiation, and only the central voxel showed a temperature change during that time, 1 mm of insulation was found to be sufficient, which also corresponds to the machining limitation for this component.

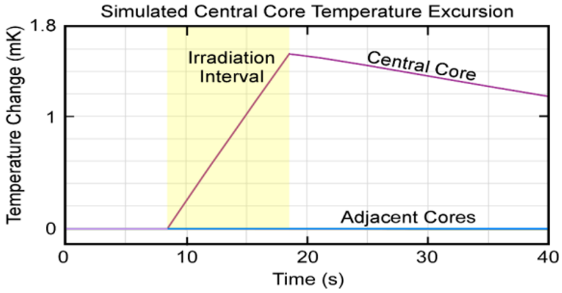

Fig. 2. Core temperature data from a simulated irradiation in COMSOL Multiphysics. Irradiation time was 10 seconds and is marked by the yellow box. Only the central voxel was irradiated and the insulation between voxels was minimized, at 1 mm for the closest points for adjacent shields. Results show that only the irradiated core experiences a temperature increase, meaning there is negligible heat flow into other cores during measurement and thus this thickness of insulation is sufficient.

3 Operational mode and electrical control system

3.1 Array operation

The calorimeter array officially operates in a quasi-adiabatic mode, although the shield independently operates isothermally. This dual-mode operation has been championed by the French national standards lab, LNHB, with their series of primary standard graphite calorimeters

[7]. The core and jacket are held in thermal equilibrium through a thermal feedback system. Thermistors in the core and jacket form legs of a Wheatstone bridge that feeds into a PID controller, which sends current as needed through a pair of heating thermistors in the jacket. Jacket heating thus maintains quasi-adiabatic conditions as the core is heated during an irradiation. The shield has a measurement thermistor that feeds into its own PID controller that is set at a constant temperature above what the ambient air could reach even if the air heats up during an irradiation. This isothermal operation prevents air fluctuations from affecting measurements and provides another barrier to heat flow between voxels.

To reduce measurement uncertainty, the measurement thermistors inside of the cores undergo an electrical calibration after the array has been constructed. Joule-heater thermistors in the cores deposit a known amount of heat into the corse. By measuring the response of the measurement thermistor, a core-specific calibration can be obtained which takes into account any heterogeneities in the core as well as the exact core geometry.

3.2 Electrical Systems

After exiting the array, thermistor leads are connected to an analog amplifier board containing necessary components for the Wheatstone bridges, noise reduction, and signal amplification. This board is itself connected to a LabJack T7 DAQ device (LabJack Corporation, Lakewood, CO). The LabJack functions as an analog-to-digital convertor for the measurement thermistors as well as the voltage supply for the Joule heaters. The LabJack is controlled by a custom Python code which writes the measurement data to a computer, runs the PID controllers, and changes the LabJack voltage outputs as needed.

4 Conclusions

The majority of primary standards labs around the world use calorimeters for absolute radiation dosimetry, but all of these calorimeters have been single-point or 1 dimensional at most. This application is the case despite most radiotherapy fields being spatially large and very heterogeneous. A nine-voxel aluminium calorimeter has been designed to obtain 2-dimensional absolute dosimetry which was primarily based on requirements on the thermal properties of the components, material machinability, and limiting the heat flow between voxels. The calorimeter array is currently being constructed for testing and comparisons against conventional dosimeters.

Any issues observed with the final product could help identify areas where improvements are needed. This could include development of new insulation materials or temperature sensors, alternative machining techniques, or less noisy electronic readout systems. All of these conditions are planned to be investigated.

Acknowledgements The authors would like to thank Leif Lervik for his insight and assistance with machining the components of the array.

Funding This research received no external funding.

Data Availability The data presented in this study is available on request from the corresponding author.

References

1. WHO Media Team, Global cancer burden growing, amidst mounting need for services, World Health Organization (2024). https://www.who.int/news/item/01-02-2024-global-cancer-burden-growing--amidst-mounting-need-for-services
2. Mayo Clinic Staff, Radiation therapy, Mayo Clinic (2024) https://www.mayoclinic.org/tests-procedures/radiation-therapy/about/pac-20385162
3. J. Renaud, H. Palmans, A. Sarfehnia, J. Seuntjens, Absorbed dose calorimetry. Phys. Med. Biol. **65**, 05TR02 (2020). https://doi.org/10.1088/1361-6560/ab4f29
4. M-A. Lebel-Cormier, T. Boilard, M. Bernier, L. Beaulieu, Multi-point calorimeter using distributed fiber Bragg gratings for small field dosimetery in radiotherapy, Med Phys, 51 **(5)**, 3758-3765 (2024) https://doi.org/10.1002/mp.16955
5. J. Renaud, A. Sarfehnia, J. Bancheri, J. Seuntjens, Aerrow: A probe-format graphite calorimeter for absolute dosimetry of high-energy photon beams in the clinical environment, Med Phys, 45 (**1**), 414-428 (2018). https://doi.org/10.1002/mp.12669
6. J. Renaud, On the Development of Absorbed Dose Calorimeter Systems for Absolute Clinical Dosimetry, Ph.D. thesis, McGill University, Department of Physics (2016)
7. J. Daures, A. Ostrowsky, B. Rapp, Small section graphite calorimeter (GR-10) at LNE-LNHB for measurements in small beams for IMRT, Metrologia, **49**, S174-S178 (2012). https://doi.org/10.1088/0026-1394/49/5/S174
8. A. Bourgouin, *et al.*, The probe-format graphite calorimeter, Aerrow, for absolute dosimetry in ultrahigh pulse dose rate electron beams, Med Phys, 49 **(10)**, 6635-6645 (2022). https://doi.org/10.1002/mp.15899
9. B. Côté, *et al.*, Feasibility of operating a millimeter-scale graphite calorimeter for absolute dosimetry of small-field photon beams in the clinic, Med Phys, 48 **(11)**, 7476-7492 (2021). https://doi.org/10.1002/mp.15244
10. J. Daures and A. Ostrowsky, New constant-temperature operating mode for graphite calorimeter at LNE-LNHB, Phys. Med. Biol. **50**, 4035-4052 (2005). https://doi.org/10.1088/0031-9155/50/17/008
11. F. M. R. Keszti, Numerical design and optimization of a millimetre-scale absorbed dose calorimeter for use in small-field megavoltage photon beams, Master Thesis, McGill University, Medical Physics Unit (2020)